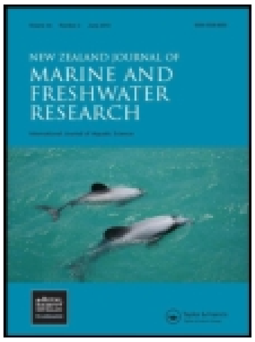


New Zealand Journal of Marine and Freshwater Research

ISSN: 0028-8330 (Print) 1175-8805 (Online) Journal homepage: http://www.tandfonline.com/loi/tnzm20

# Locally generated tsunami along the Kaikoura coastal margin: Part 2. Submarine landslides

Roy Walters , Philip Barnes , Keith Lewis , James R. Goff & Jason Fleming

**To cite this article:** Roy Walters , Philip Barnes , Keith Lewis , James R. Goff & Jason Fleming (2006) Locally generated tsunami along the Kaikoura coastal margin: Part 2. Submarine landslides, New Zealand Journal of Marine and Freshwater Research, 40:1, 17-28, DOI: 10.1080/00288330.2006.9517400

**To link to this article:** http://dx.doi.org/10.1080/00288330.2006.9517400

0028–8330/06/4001–0017 

# Locally generated tsunami along the Kaikoura coastal margin: Part 2. Submarine landslides

ROY WALTERS[1]
PHILIP BARNES[2]
KEITH LEWIS[2]
JAMES R. GOFF[1]
JASON FLEMING[1]

[1]National Institute of Water and Atmospheric Research Limited
P.O. Box 8602
Christchurch, New Zealand
email: r.walters@niwa.co.nz

[2]National Institute of Water and Atmospheric Research Limited
Private Bag 14901
Wellington, New Zealand

**Abstract** An examination of the underwater landscape along the northeast coast of the South Island, New Zealand, identified a substantial potential for a submarine landslide in Kaikoura Canyon. A numerical model was applied to calculate runup and inundation arising from a local tsunami generated by such a landslide. The model is based on the Reynolds-averaged Navier-Stokes (RANS) equation and used a finite element spatial approximation, implicit time integration, and a semi-Lagrangian advection approximation. The results indicate that a landslide-generated tsunami represents a large potential hazard to the area from South Bay to Oaro, South Island, New Zealand, and has the potential to generate large tsunami runup heights along this section of coast. In addition, the tsunami events are characterised by a short time interval between generation and runup.

**Keywords** tsunami; submarine landslide; Kaikoura Canyon; New Zealand

*M05023; Online publication date 31 January 2006*
*Received 28 April 2005; accepted 7 September 2005*

## INTRODUCTION

Submarine canyons are a common, almost ubiquitous feature of the world's continental margins (Shepard 1981). They are sites of slope failure, and have been cut into continental slopes by a number of mass failure processes. These processes include turbidity currents, which are infrequent but generally catastrophic, high density, high velocity, turbid flows of gravel, sand and mud. In this paper, the focus is on locally generated tsunami resulting from submarine landslides in Kaikoura Canyon (Fig. 1). The tectonic setting for this study was described in Part 1 of this study (Walters et al. this issue), where the focus was on tsunami generated by local fault ruptures associated with submarine earthquakes.

There are no unequivocal historically documented accounts of canyon-related tsunami in this region. Similarly, geological evidence is sparse at best, although this is not entirely surprising given that no specific palaeotsunami studies have been carried out. In the archaeological literature however, there are some possible indications of marine inundation. Marine sediments overlie a Maori occupation site on Seddon's Ridge, overlooking South Bay (Fig. 2) (Duckmanton 1974). This indicates inundation by the sea sometime within the last 150–200 years. At the western end of South Bay a similarly dated disturbance of a Maori occupation site was also noted, with water-worn pebbles mixed with artefacts (Fomison 1963). Seddon's Ridge, an uplifted beach ridge, has a long history of Maori settlement. An older village site (c. 650 years BP) here, c. 350 m from the sea, contains reworked oven stones and is overlain by marine overwash deposits (Duckmanton 1974; Boorer 2002). In the absence of geological data, this kind of archaeological information is only circumstantial. However, it does at the very least indicate that the sea has overtopped past coastal settlements in the region as a result of a severe storm surge or tsunami. This signals the need for further research.

The following section of this paper summarises background information on Kaikoura Canyon and

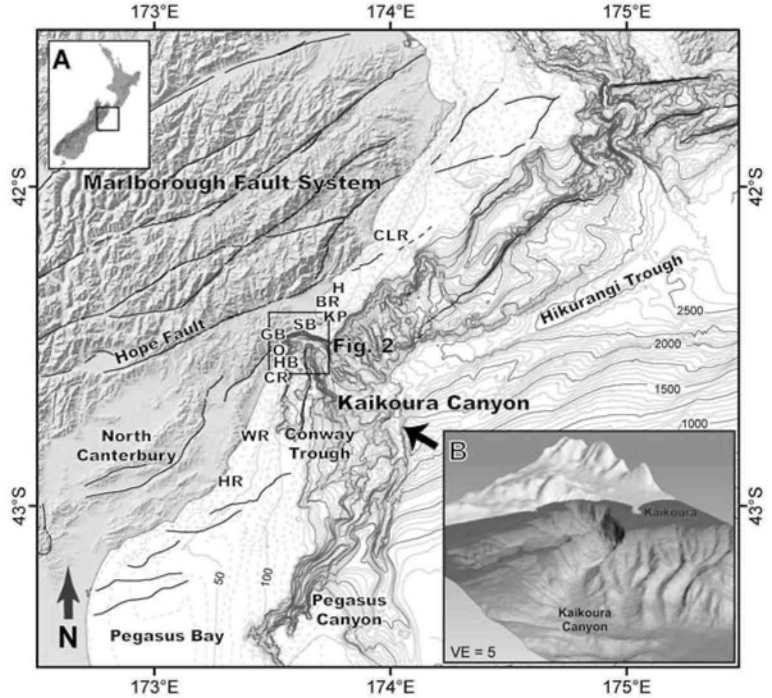


**Fig. 1** Offshore bathymetry of the Kaikoura margin and hillshade model of land topography (main figure). Bathymetric contours are in metres. Black lines are simplified tectonic faults. (CLR, Clarence River; H, Hapuku; BR, Beach Road; KP, Kaikoura Peninsula; SB, South Bay; GB, Goose Bay; O, Oaro; HB, Haumuri Bluffs; CR, Conway River; WR, Waiau River; HR, Hurunui River.) Inset A shows general location. Inset B is an oblique view of a 3-dimensional bathymetric model of Kaikoura Canyon viewed in the direction of the bold arrow on the main map.

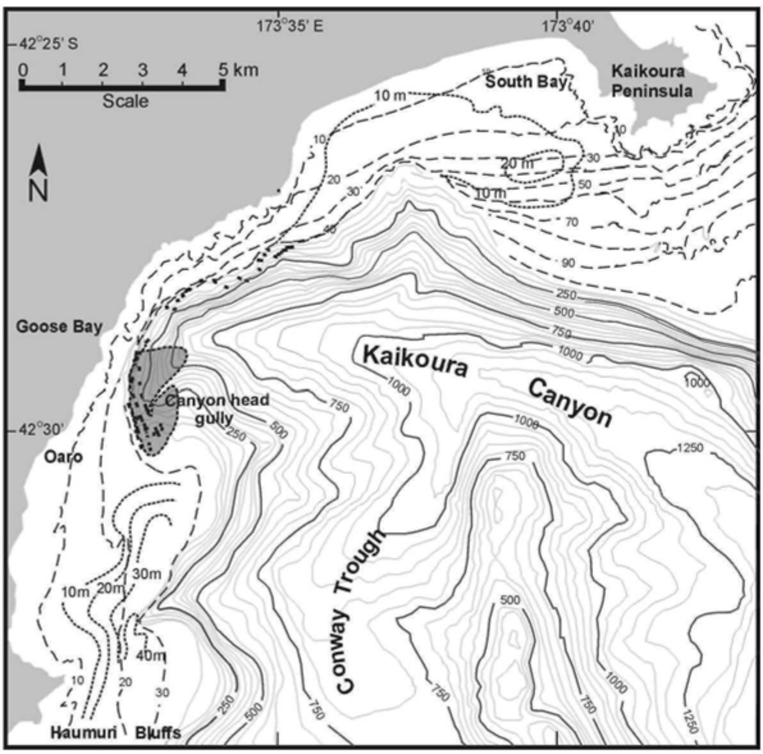


**Fig. 2** Bathymetric map of the upper reaches of the Kaikoura Canyon, New Zealand. Bathymetric contours (solid lines) are at 50-m intervals on the slope. Selected contours at 10-m intervals are shown on the shelf as dashed lines. Fine dotted lines are contours of the thickness of post-glacial (<12 ka) sediment on the shelf. Bold marks in shaded area are inferred slump scarps developed in the post-glacial sediments. Shaded area is inferred to be the area susceptible to a potential future landslide event.

the potential for submarine landslides that can be a significant mechanism for tsunami generation (Lewis & Barnes 1999). We then describe the numerical model for surface waves and the submarine landslide submodel that were used in this study. Then we present a case study of local tsunami generated by a landslide scenario at the head of the canyon.

## KAIKOURA CANYON

The Kaikoura coastline straddles an area with substantial vertical topographic and bathymetric relief, as well as considerable geological complexity (Fig. 1). The submarine trench marking the edge of the plate boundary, the Hikurangi Trough, shallows southwards along the toe of the Marlborough continental margin, and terminates in c. 2500 m water depth at a location c. 40 km offshore of Kaikoura Peninsula. At the southern end of the Hikurangi Trough, major submarine canyons incise the continental margin and are conduits for sediment transport from the Southern Alps to the Hikurangi Trough and beyond to the deep Pacific Basin (Lewis 1994; Lewis et al. 1998). Some, such as Pegasus Canyon, have not been significantly active since 18 ka BP, when last-glacial shorelines supplied sediment to the canyon head (Herzer 1981). In contrast, the Kaikoura Canyon is presently active because it intersects the modern sediment transport system in the nearshore region (Lewis & Barnes 1999). It is the potential instability of sediment at the head of this canyon that is of interest to this tsunami study.

Kaikoura Canyon owes much of its special character to its position within the centre of the convergent boundary between Pacific and Australian plates (Fig. 1). The canyon lies in a transition zone between the Hikurangi subduction system to the northeast and the oblique continental collision of the Southern Alps to the southwest. There is rapid uplift of coastal ranges near Kaikoura as a result of active strike-slip and thrust faults within the Marlborough Fault System and North Canterbury (Fig. 1). One of the major strike-slip faults, the Hope Fault, lies immediately north of Kaikoura and is commonly depicted as the main plate boundary fault (Fig. 1).

Kaikoura Canyon is unusual in several ways. First, it is one of the few active canyons that are not close to the mouth of a sediment-charged river. The canyon does, however, receive abundant sediment from the south via long-shore drift systems and strong currents (Carter & Herzer 1979). Second, it is incised 600–1200 m into the adjacent shelf and slope, and cuts across almost the entire shelf to nearly intersect the present coast. Offshore from Goose Bay south of Kaikoura, the canyon comes to within 200 m of the coast and the canyon rim is 18–34 m deep (Fig. 2). Its head is well within the zone where modern sediments from rivers to the south are moved northwards by southerly storms. Unlike most of the world's canyons, it has been highly active over the last few millennia (Lewis & Barnes 1999). Third, the upper reaches of the canyon intersect an 8 km by 30 km rectangular fault-controlled depression (Conway Trough) in the north Canterbury shelf. Finally, the canyon is unusual in that instead of depositing most of its sediment load as a fan at the base of the slope, it merges into a 2000 km long, meandering, deep-sea channel (the Hikurangi Channel) that distributes sediment from Kaikoura over vast areas to the northeast. This sediment distribution probably requires catastrophic inputs from avalanches rather than much more frequent storm-generated grain flows (Lewis et al. 1998).

### Size and shape

The Kaikoura Canyon is 60 km long and follows a broad curve from the narrow, mountain-backed shelf off Goose Bay to the 2000 m deep apex of the Hikurangi Trough. Off Goose Bay, the canyon falls from near the coast to the 600 m deep floor of the canyon within c. 1 km. This 25–30° slope is the left wall of a narrow, steep-sided, V-profiled, canyon-head gully that extends southwards sub-parallel with the coast, for c. 3 km towards Oaro (Fig. 2). The axis of the gully slopes at c. 12° between the 32 m and 600 m isobaths. High frequency (3.5 kHz) seismic profiles of the steep-sided canyon-head appear to reveal chaotic sediment infill that is at least 70 m thick in the upper gully decreasing to c. 20 m thick in the lower gully (Lewis & Barnes 1999).

The upper canyon, from the 600 m isobath off Goose Bay to the 1300 m isobath, obliquely incises the continental shelf for 14 km. It has a U-shaped profile and its steep northern (left) wall is 1000–1200 m high with average slopes of 20–30° and cliffs of more than 45°. Above the confluence with Conway Trough, the canyon-floor is 300–700 m wide with a few tens of metres of parallel-bedded, sandy turbidites and an axial slope of c. 4°. Below the confluence with the Conway Trough, the slope is only 1.5° and the broadly U-shaped floor reaches 1.5 km wide near the 1250 m isobath.

The central section of the canyon below the 1300 m isobath contains a slump deposit estimated to be over 200 m thick and to cover an area of c. 8 km$^2$ (Lewis & Barnes 1999). Below the slump deposit the lower canyon continues in a broad curve into the upper end of the Hikurangi Trough at a slope of 1.5° to 0.5°. The lower canyon walls are more gently sloping, and there is no evidence of significant slope failure there.

**Sediment supply**

The rivers of eastern South Island supply over $30 \times 10^6$ m$^3$ of sediments to the Pacific Ocean each year (Carter et al. 1982; Carter & Herzer 1979). When the sediment reaches the coast, gravel, sand and mud are loosely split into three fractions. Gravel and coarse sand remain mainly within the surf zone, medium and fine sand moves to the inner shelf, and mud settles mainly on the mid to outer shelf and beyond. This input contributes to nearshore and mid shelf sediment prisms, and a major part of each fraction is moved northwards by wave action, southerly swells, tides and the weak Southland Current (Carter et al. 1982; Carter & Herzer 1979).

Lewis & Barnes (1999) discussed the annual sediment budget supplied to the head of Kaikoura Canyon. The northeastward-moving, inner shelf sediment transport system that ends at Kaikoura Canyon, begins immediately north of Pegasus Bay, and includes the inputs from the Hurunui, Waiau, and Conway rivers (Carter et al. 1982). These rivers supply an estimated $5 \times 10^6$ m$^3$ of sediment each year (5 km$^3$/ka) to this system (Griffiths & Glasby 1985). Of this, only c. 0.1–$0.2 \times 10^6$ m$^3$ per year is gravel, c. $2 \times 10^6$ m$^3$ per year is sand, and c. $3 \times 10^6$ m$^3$ per year is mud (Carter et al. 1982). The gravel tends to be confined within beach compartments by headlands, notably Haumuri Bluffs, and most of the mud is swept offshore and deposited as "hemidetrital" drape on the continental slope and in deep-sea troughs. The $2 \times 10^6$ m$^3$ per year of sand forms the dominant component of the shelf sediment transport system (Lewis & Barnes 1999).

Off Haumuri Bluffs, the zone of northward-moving fine sand is c. 3 km wide and high-resolution seismic profiles show that the modern (post last glacial) sediment prism is a maximum of 40 m thick (Lewis & Barnes 1999). Assuming that the modern sediment prism has a similar profile along the 50 km of shelf between the most southerly sediment-supply river and the canyon head, it is estimated that the volume of modern sediments on the shelf is c. 3 km$^3$, mostly of sand (Lewis & Barnes 1999). This is equivalent to the total river input for 600 years or the sand input for 1500 years. Since deposition on the inner shelf transgressive erosion surface began between c. 12 000 years ago at the outer edge of the prism and c. 6000 years ago at the present coast, over 90% of total river input and over 75% of all river sand (no allowance being made for coastal erosion or higher inputs in cooler conditions) has disappeared from the shelf. Estimates for the late Holocene (based on thickness above an inferred mid Holocene reflector) are similar within the accuracy of the methods (Lewis & Barnes 1999). Thus, of the c. $2 \times 10^6$ m$^3$ of sand that is input each year, an estimated $0.5 \times 10^6$ m$^3$ builds up the shelf sediment prism and c. $1.5 \times 10^6$ m$^3$ per year is lost from the shelf. Lewis & Barnes (1999) inferred that much of the latter falls into the head of the Kaikoura Canyon.

The canyon-head gully of Kaikoura Canyon is positioned to trap a major part of the mobile sand and silt that bypasses Haumuri Bluffs. The head of the gully intersects the thickest part of the shelf sediment prism whereas the left wall of the gully intersects the most mobile part of the sediment transport system. Coarse sand and gravel are input where the western wall of the gully incises these sediment types near Goose Bay. In certain hydrological conditions, sediment from the south pours into the canyon-head gully, where it has accumulated a thickness of at least 70 m (Lewis & Barnes 1999).

Although the existing seismic reflection coverage is inadequate to precisely define the full extent and volume of the deposit, sidescan sonographs provided additional evidence, showing three lines of incipient failure scarps, c. 180 m apart and 1–2 km long, around the head and western wall of the gully (Lewis & Barnes 1999). These were inferred to define the top and inner edge of the sediment prism. Rough estimates using the limited data set suggested a volume of the gully-head sediment prism in the order of $240 \times 10^6$ m$^3$ (0.24 km$^3$). If c. $1.5 \times 10^6$ m$^3$ of sediment pours into the canyon head each year, then the present sediment pile has accumulated in c. 160 years. Considering the accuracy of the estimates, the present prism might have accumulated in c. 100–300 years, rather than in tens or thousands of years. This clearly indicates that the sediment in the canyon head gully has flushed down the canyon within the last few hundred years.

**Potential catastrophic failure in the canyon head**

Rapidly accumulating sandy sediment on a steep slope, in an active tectonic region, is likely to be susceptible to failure during the undrained cyclic loading that can be expected in moderately large earthquakes (Lee & Edwards 1986). Frequent strong ground shaking associated with rupture on nearby faults can be expected to reduce the shear strength of the sandy sediment prism and may trigger mass failures. That such failures have occurred often in the Kaikoura Canyon is evidenced by the occurrence of numerous sand and gravel turbidite deposits in cores from the canyon axis (Lewis & Barnes 1999).

The return period for major (magnitude 8) earthquakes at Kaikoura has been estimated to be in the order of a century or two (Van Dissen 1991) based mainly on knowledge of plate boundary faults close to Kaikoura. Stirling et al. (2001) estimated a peak ground acceleration at Kaikoura township of 0.44 *g* for a return period of 150 years. There have been no large seismic events centred close to Kaikoura since written records of the area began in about 1840 AD, but lichen-dating of rock-falls suggests that there may have been a major earthquake in the vicinity c. 175 years ago (Bull & Brandon 1998). This is approximately the time taken to accumulate the present sediment deposits observed in the canyon head. We can speculate therefore that sediment in the canyon head gully failed and flowed down the canyon as a major turbidity current released by this earthquake.

There is some tentative confirmation for this in the dating of twigs in the top two gravel turbidite deposits in the lower canyon (Lewis & Barnes 1999). A twig in the lower layer has been radiocarbon dated at 251 ± 64 BP with a calibrated age range of 1470–1960 AD (Lewis & Barnes 1999). The age of the twig in the upper gravel layer (122 ± 85 BP) has a calibrated age of 1650–1960 AD (95% probability). If, indeed, failure is triggered by major earthquakes (which have not been recorded in the Kaikoura area since European settlement in c. 1840), then the top gravel is probably older than c.1840 AD. The lower gravel layer must be older than this but there is insufficient data to determine the precise age. However, there would need to be sufficient time to accumulate a deposit at the canyon head. This evidence on timing and frequency is circumstantial, but is the best estimate at the present time. We can speculate that the recurrence interval of major turbidites is of the same order of magnitude as the estimated return time of major earthquake ground shaking at Kaikoura given by Van Dissen (1991) and Stirling et al. (2001). The only other corroborative evidence is that turbidites are deposited in the central Hikurangi Trough 300 km to the northeast once every few centuries (Lewis 1994).

If it takes a century or so to accumulate enough sediment in the canyon head gully to generate a major mass failure and turbidity current, then there is already enough sediment to pose a hazard. Tensional cracks at the head of the modern deposit (Lewis & Barnes 1999) indicate that it is likely to fail as a result of ground shaking associated with a future major earthquake. Failure would result in the catastrophic collapse of about a quarter of a cubic kilometre of unconsolidated sediment with its top in 34 m of water and its base c. 450–500 m deep. In most canyons elsewhere, such failures are directed away from the coast. Collapse in the canyon-head gully of the Kaikoura Canyon differs in that the head of the gully faces northwards, obliquely towards the shore. Thus, initial motion of a debris avalanche in the gully, and the potential resulting tsunami, is towards the shore of South Bay and the southern side of Kaikoura Peninsula.

## MODEL DESCRIPTION

A numerical model was used to simulate the behaviour of a submarine landslide and the subsequent generation, propagation, and runup of a tsunami. The numerical model is a general-purpose hydrodynamics and transport model known as RiCOM (River and Coastal Ocean Model) that is based on the Reynolds-averaged Navier-Stokes equations (RANS) with a free surface (Walters & Casulli 1998; Walters 2004, 2005a,b). The hydrodynamics part of this model was used to derive the results described in the next section (described in more detail in Part 1 (Walters et al. this issue).

To accommodate submarine landslides, additional terms were introduced into the equations to account for a time-dependent bottom elevation. Toward this end, the kinematic boundary condition at the bottom was modified to include vertical movement of the sea floor:

$$\frac{D(h-z)}{Dt} = \frac{\partial h}{\partial t} + \mathbf{u}\cdot\nabla h - w_h = 0 \qquad (1)$$

where $D/Dt$ is a material derivative, $h(x,y,t)$ is land elevation measured from the vertical datum, $z$ is the vertical coordinate, $\mathbf{u}$ is horizontal velocity, $\nabla$ is the horizontal gradient operator, and $w_h$ is vertical velocity at the bottom.

The free surface equation is derived from vertically integrating the continuity equation and using the kinematic boundary conditions:

$$\frac{\partial \eta}{\partial t} + \nabla\cdot(H\mathbf{u}) = \frac{\partial h}{\partial t} \qquad (2)$$

where $\eta(x,y,t)$ is the water-surface elevation measured from the vertical datum, and $H = \eta(x,y,t)-h(x,y,t)$ is the water depth.

In essence, an extra source term was added to the free surface equation and the governing equations were solved in the same manner as before. In practice, $h(x,y,t)$ was calculated in a separate landslide submodel followed by calculation of the free surface elevation for each time step.

**Submarine landslide submodel**

Modelling the dynamics of submarine landslides (a mixture of fluid and sediments) and the coupled generation of surface waves is a complicated scientific problem that has not yet been solved adequately. The movement of submarine landslides is controlled by a complicated interaction between sediment particles and the modification of these interactions by the interstitial fluid (Iverson & Denlinger 2001). The subsequent deformation of the air/water surface is owing to the incompressibility of water and to a dynamic response to the pressure field that has been modified by the landslide (Jiang & LeBlond 1994; Rzadkiewicz et al. 1997; Liu et al. 2005). As the landslide moves under the influence of gravity, water is entrained, altering the properties of the sediment, and this may lead to the generation of turbidity currents. These effects and the formation of complex interfaces between turbidity currents and surrounding still water can further complicate the dynamics.

Underwater landslides are in a sense similar to the class of granular material phenomena exemplified by water-saturated debris flows (Iverson & Denlinger 2001). Here the granular material moves downslope under the influence of gravity, while pressurised by water at nearly hydrostatic pressure. The dynamics are characterised by grain-grain and grain-fluid interactions while moving over three-dimensional topography.

Until recently, there has been no satisfactory theory to quantify these dynamics. Research has been based on the assumption of a viscous or viscoplastic fluid where the focus was on the development of empirical formulas for the landslide rheology (Jiang & LeBlond 1993, 1994; Rzadkiewicz et al. 1997). However, establishing values for the various empirical parameters presents a fundamental problem for prediction.

On the other hand, recent advances using mixture theory have led to spectacular success in the analysis of dry granular avalanches and water-saturated debris flows (Iverson & Denlinger 2001; Denlinger & Iverson 2001). Here, the theory explicitly accounts for fluid-phase and solid-phase forces and interactions using Coulomb mixture theory (Savage & Hutter 1989; Iverson 1997; Iverson & Denlinger 2001). The governing equations reduce to standard equations for mass and momentum conservation with sediment and fluid forces entering through the stress terms. The sediment stresses include intergranular interactions and the effects of pore pressure.

Several conceptual approaches to describe submarine landslides are possible, including: (1) solid blocks that represent the landslide volume sliding down inclined surfaces as an approximation in themselves or used to generate wavemaker curves in laboratory experiments (e.g., Watts 1998; Watts et al. 2000); (2) a viscous Newtonian sediment (e.g., Jiang & LeBlond 1993, 1994; Rzadkiewicz et al. 1997); (3) mixture theory which includes the effects of Coulomb forces (Denlinger & Iverson 2001); and (4) particle dynamics that consider individual particles interacting in a viscous fluid (Cundall & Strack 1979).

Our approach has been to sequentially develop models based on concepts 1 to 3, each built on knowledge gained from the previous example. Approach 4 is too computationally intensive to be used in field-scale applications and hence is eliminated at the outset. Results from approach 2 indicated that the sediment/fluid/water surface interaction is too complicated to be represented by solid blocks that are difficult or impossible to implement in irregular 3-dimensional terrain. Hence, approach 1 was also not considered. At this stage, we have developed a depth-integrated viscous Newtonian sediment model with basal slip and friction. This model approximates the dynamics of a landslide after it becomes fluidised, and the basal slip represents the effects of a bottom shear layer. As the basal stress becomes small, the dynamics approximate hydroplaning.

We also developed a preliminary model using mixture theory based on the work of Iverson & Denlinger (2001) and Denlinger & Iverson (2001). This model has the advantage that it includes Coulomb friction and is being developed and tested using a series of laboratory experiments with submarine landslides (Fleming et al. 2005).

As a consequence, the submarine landslide model used in this study was based on the shallow water equations and approximated a viscous Newtonian fluid with a bottom shear layer. The equations and solution methods were the same as the model for the overlying fluid which is described in Part 1 (Walters et al. this issue) and in Walters & Casulli (1998).

**Model grid and bathymetry**

The bathymetric data were compiled from several sources as described in Part 1 of this paper. From this data, a finite element model grid was generated using triangular elements. The grid contained both

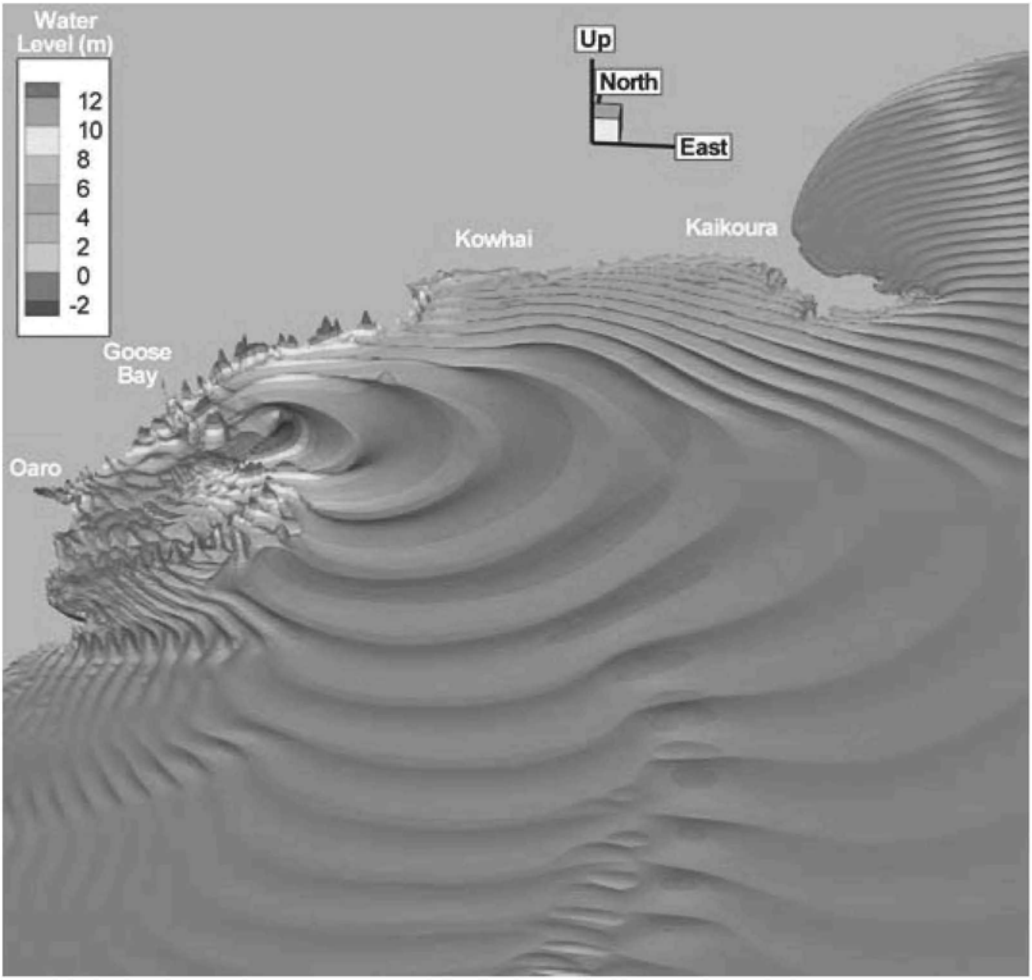


**Fig. 3** Time sequence of water surface elevations at 30-s intervals.

the coastal ocean and a land grid with elevations up to c. 20 m above mean sea level (MSL).

### Landslide geometry

The volume of the present head-gully sediment prism capable of potential mass failure is in the order of $240 \times 10^6\,m^3$ ($0.24\,km^3$) (Lewis & Barnes 1999). As a case study of a potential scenario, we used this volume estimate, combined with the bathymetric data, to construct a pre-landslide and hypothetical post-landslide topography assuming that catastrophic failure of the sediment prism occurs (Fig. 2). The pre-landslide topography is identical to the reference topography that was interpolated onto the model grid. We also used a secondary model grid that contains the post-landslide topography. Both grids were used within the model to define the initial bottom topography, the mass that fails and starts sliding down the head of the canyon, and the final topography of the canyon head gully after failure. The movement of the landslide was governed by the landslide model described earlier.

## RESULTS AND DISCUSSION

The modelled submarine landslide occurred directly offshore from Goose Bay and affected primarily Oaro to South Bay (Fig. 3). For this event, the source area was much smaller than for the fault displacement events considered in Part 1 (Walters et al. this issue, fig. 4). Hence, the effects were primarily felt locally and the wave dissipated fairly rapidly. This was balanced by the wave amplitudes being much larger than for the fault dislocation example and the source being close to the coast (Fig. 3).

When a landslide occurs, the water above the landslide is drawn down by the sinking mass and the water in the direction of movement forms a forced wave (like a bow wake) that is pushed along at the speed of the landslide (Watts et al. 2000; Fleming et al. 2005; Liu et al. 2005). In deep water, the leading wave is less developed. When the landslide changes direction or moves more slowly than the phase speed of surface wave, the forced wave becomes a freely propagating wave. For Kaikoura Canyon, it is significant that the direction of landslide movement and forced wave propagation is toward South Bay rather than toward the open ocean.

The effects of a submarine landslide are strongly dependent on the size and water depth of the landslide and on the density of the landslide material (Watts 1998; Liu et al. 2005). As the size increases and the water depth decreases, the landslide will create a larger depression in the overlying water. Water propagates into the depression with the phase speed

$$c = \sqrt{\frac{g}{k}\tanh(kH)}$$

where $g$ is gravitational acceleration and $k$ is wavevector. For shallow water waves this reduces to $c = \sqrt{gH}$. Hence as area increases, there is a greater distance to propagate and, as $H$ decreases, the wave propagates more slowly. In addition, the acceleration of the landslide is dependent on the driving force $g[(\rho_s - \rho_w)/\rho_w]\sin\alpha$ where $\rho_s$ is the sediment density, $\rho_w$ is the water density, and $\alpha$ is the bottom slope. As the sediment density increases, the acceleration of the landslide and the amplitude of the surface wave increase.

As part of the evaluation of the results, the grid resolution and the time step size were varied so as to verify that the model had converged to an accurate solution. In addition, we performed sensitivity tests on the parameters controlling landslide acceleration.

The landslide acceleration was an important factor in the results and was dependent on the specific density of the submerged landslide mass and friction with the underlying solid bed. The two adjustable parameters in this submodel were the coefficient $C_L$ for linear basal friction (equivalent to $\gamma$ in equation 3 of Part 1) and the landslide density $\rho_s$. Sensitivity tests were used to assess the dependence of the acceleration, and hence surface wave amplitude, on an estimated range of densities for the continental shelf around Kaikoura, and on an estimated range of friction parameters. The specific density can vary from 1200 kg/m$^3$ (low density unconsolidated surface sediments) to 2000 kg/m$^3$ (highly consolidated sediment) (Keller & Bennett 1970; Barnes et al. 1992; US Army Corps of Engineers 1998). The friction parameter in the model was varied from 0.1/s (high friction adhesion) to 0.001/s (low friction slipping). A friction parameter of 0 corresponds to a landslide hydroplaning with no bottom friction. Our best estimate for these parameters was 1600 kg/m$^3$ for the density and 0.02 s$^{-1}$ for the friction coefficient. This estimate was based on reproducing reasonable landslide dynamics that were consistent with laboratory experiments (Fleming et al. 2005) and with field evidence for turbidity currents (Lewis & Barnes 1999).

The sequence of events during the generation and propagation of the tsunami is illustrated in Fig. 3, where snapshots of surface elevation at 30-s intervals are superimposed. The simulation started with an undisturbed water surface at MSL. When the landslide started, the sediments on the steep sides of Kaikoura Canyon moved downslope to the deeper canyon axis. Along the canyon axis the landslide was moving more slowly because of the smaller bottom slope. The net effect was that a depression in the water surface forms along the sides of the canyon, a higher water surface elevation forms over the canyon, and a forced wave forms at the lower end of the canyon in the direction of landslide movement (Fig. 3, centre of wave pattern). After this initial period, the main landslide moved more slowly than the surface wave speed (order of 10 m/s as opposed to 20 to 100 m/s) so that the initial surface wave was radiated away as a free wave. The initial wave near Goose Bay is readily apparent in Fig. 3, as are the curved wave crests propagating towards South Bay and around Kaikoura Peninsula. The resultant tsunami was primarily localised to the area from Oaro to South Bay, with the largest effects at Goose Bay. In addition, there was refraction of the wave around Kaikoura Peninsula and propagation northward along the coast.

The results presented here were for an average rather than a worst-case scenario. For the average example, the initial sea level was at MSL, landslide density was taken as 1600 kg/m$^3$, and the friction coefficient was taken as 0.02 s$^{-1}$. Results for the

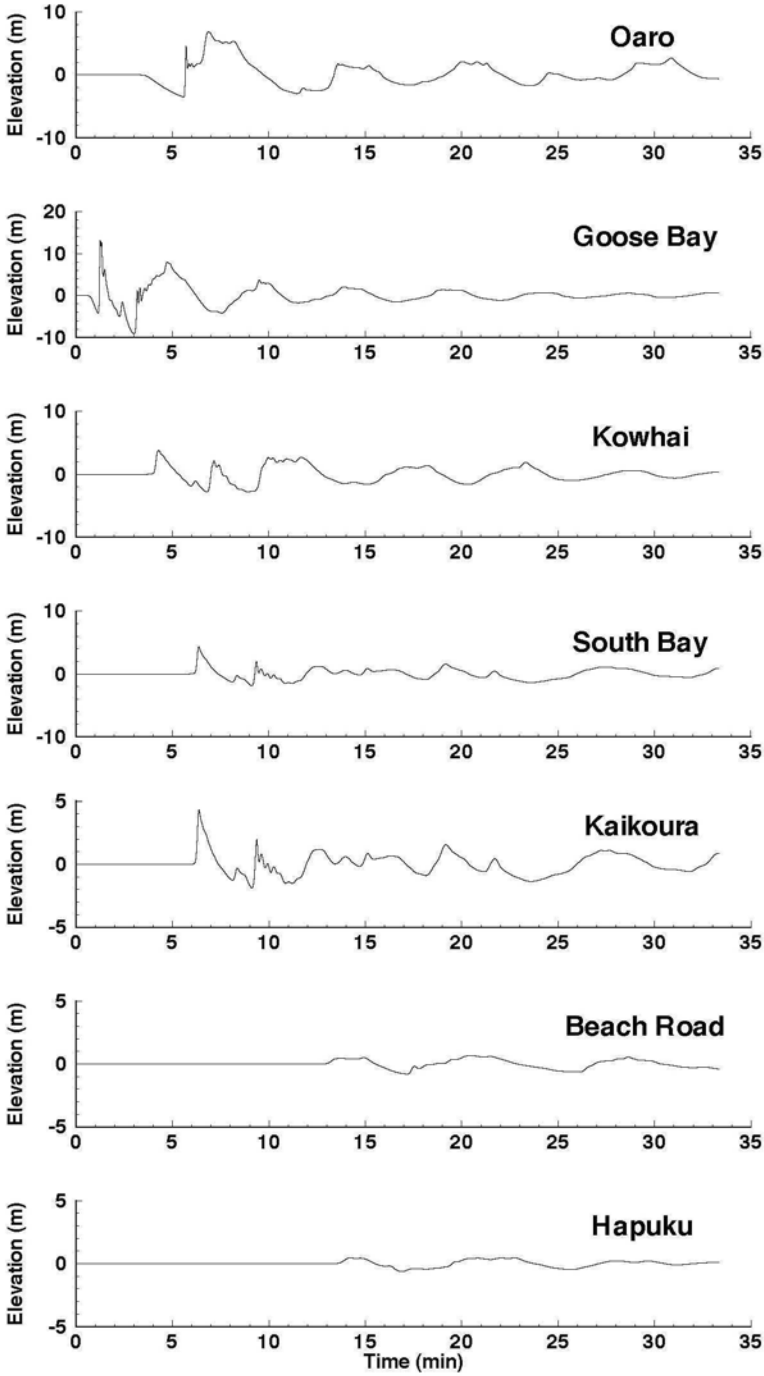


**Fig. 4** Time series of water elevation at the model recording sites. Note change in vertical scale in the plots.

worst-case scenario are presented in Walters et al. (2004).

For the average-case scenario, the incident wave at Goose Bay arrived c. 1 min after the event started, had a wave crest height of c. 13 m above the tide level, and the runup height was over 20 m above the tide level (Fig. 4). There was complete inundation of the road bed and low lying areas at Goose Bay.

The wave then propagated south towards Oaro and north towards South Bay. Between Goose Bay and South Bay, the wave crest swept down the coastal cliffs with a relatively large runup height. After passing the end of the cliffs, the wave spread out over the beach and the low lying areas farther north. Slightly smaller waves arrived at Oaro 3 min and South Bay 7 min after the landslide started but were still sufficiently large to inundate most of the coastal platform. At Kaikoura, the wave arrived at c. 15 min after the landslide started and had a wave crest height of slightly less than 2 m. A sequence of waves persisted at Kaikoura for the next 50 min. Two waves converged at Hapuku a few minutes after the wave passed Kaikoura, resulting in a wave crest height of over 1.5 m. North of Hapuku, the wave heights were generally small.

For the worst-case scenario, the initial sea level was at high water for spring tides (0.83 m) plus a maximum storm surge (0.5 m) which gave an initial value of 1.33 m, landslide density was taken as 1800 kg/m$^3$, and the friction coefficient was 0.01 s$^{-1}$ (Walters et al. 2004). The maximum wave heights for the worse case were higher by 1.33 m plus a somewhat higher wave (about 15%).

## CONCLUSION

A landslide-generated tsunami represents a large potential hazard to the area from South Bay to Oaro. An extreme event was modelled as a failure of the entire landslide mass identified in Lewis & Barnes (1999). These simulations, supported by sensitivity tests and basic analysis, indicate the potential for large tsunami runup heights along this section of coast. The effects could be under-estimated here if such an event coincided with storm activity or high tides.

An important question is whether a landslide of this magnitude could actually occur. There is sufficient anecdotal evidence that smaller slides have occurred (Lewis & Collot 2001). There is also archaeological evidence that may point to large events, but this is not certain. In light of the potential hazard and large uncertainties in recurrence, a search for field evidence requires further investigation.

In addition, the tsunami scenarios are characterised by short response times. For the landside example, there may be an earthquake pre-cursor or none, and the wave would arrive 1–3 min later at several locations.

Finally, there could be multiple-related hazard events (probably the most likely case). For instance a locally-generated tsunami could occur shortly after a local earthquake, and there could be multiple tsunami generated by both a fault rupture and underwater landslides.

## ACKNOWLEDGMENTS

This research was partially funded by the New Zealand Foundation for Research, Science and Technology under contract CO1X0024 and a Marsden Grant administered by the Royal Society of New Zealand under contract 01-NIW-101. The application of this research to the assessment of tsunami hazards along the Kaikoura coast was partially funded by Environment Canterbury (Ecan).

## REFERENCES

Barnes PM, Cheung KC, Smits AP, Almagor G, Read SAL, Barker PR, Froggatt P 1992. Geotechnical analysis of the Kidnappers Slide, upper continental slope, New Zealand. Marine Geotechnology 10: 159–188.

Boorer S 2002. Geomorphic evolution of the South Bay coast, Kaikoura. Unpublished MSc thesis, University of Canterbury, Christchurch, New Zealand. 169 p.

Bull WB, Brandon MT 1998. Lichen dating of earthquake-generated regional rockfall events, Southern Alps, New Zealand. Geological Society of America Bulletin 110: 60–84.

Carter L, Herzer RH 1979. The hydraulic regime and its potential to transport sediment on the Canterbury continental shelf. New Zealand Oceanographic Institute Memoirs 83. 33 p.

Carter L, Carter RM, Griggs GB 1982. Sedimentation in the Conway Trough, a deep near-shore marine basin at the junction of the Alpine transform and Hikurangi subduction plate boundary, New Zealand. Sedimentology 29: 475–497.

Casulli V 1999. A semi-implicit finite difference method for non-hydrostatic, free-surface flows. International Journal of Numerical Methods in Fluids 30: 425–440.

Collot J-Y, Delteil J, Lewis KB, Davy B, Lamarche G, Audru J-C, Barnes P, Chanier F, Chaumillon E, Lallemand S, Mercier De Lepinay B, Orpin A, Pelletier B, Sosson M, Toussaint B, Uruski C 1996. From oblique subduction to intra-continental transpression: structures of the southern Kermadec–Hikurangi margin from multibeam bathymetry, side-scan sonar and seismic reflection. Marine Geophysical Researches 18: 357–381.

Cowan HA 1990. Late Quaternary displacements on the Hope Fault at Glynn Wye, North Canterbury. New Zealand Journal of Geology and Geophysics 33: 285–293.

Cundall PA, Strack OD 1979. A discrete numerical model for granular assemblies. Geotechnique 29(1): 47–65.

Davey FJ, Hampton M, Childs J, Fisher MA, Lewis KB, Pettinga JR 1986. Structure of a growing accretionary prism, Hikurangi margin, New Zealand. Geology 14: 663–666.

de Lange WP, Fraser RJ 1999. Overview of tsunami hazard in New Zealand. Tephra 17: 3–9.

de Lange WP, Healy TR 1986. New Zealand tsunamis 1840–1982. New Zealand Journal of Geology and Geophysics 29: 115–134.

Denlinger RP, Iverson RM 2001. Flow of variably fluidized granular masses across 3D terrain: 2. Numerical predictions and experimental tests. Journal of Geophysical Research 106(B1): 553–566.

Duckmanton NM 1974. The shore platforms of the Kaikoura Peninsula. Unpublished MA thesis, University of Canterbury, Christchurch, New Zealand. 136 p.

Eberhart-Phillips D, Reyners M 1997. Continental subduction and three-dimensional crustal structure: the northern South Island, New Zealand. Journal of Geophysical Research 102: 11 843–11 861.

Fleming J, Walters R, Sue L, Nokes R 2005. Experimental design for solid block and granular submarine landslides: a unified approach. In: Satake K ed. Tsunamis: case studies and recent developments. Advances in Natural and Technological Hazards Research 23. Dordrecht, Springer. Pp. 259–277.

Fomison T 1963. Excavations at South Bay Kaikoura—Site S49/43. New Zealand Archaeological Association Newsletter 8: 100–102.

Griffiths GA, Glasley GP 1985. Input of river-derived sediment to the New Zealand continental shelf: 1 Mass. Estuarine Coastal Shelf Science 21: 733–787.

Herzer RH 1981. Late Quaternary stratigraphy and sedimentation of the Canterbury continental shelf, New Zealand. New Zealand Oceanographic Institute Memoir 89. 71 p.

Iverson RM 1997. The physics of debris flows. Revues in Geophysics 35: 245–296.

Iverson RM, Denlinger RP 2001. Flow of variably fluidized granular masses across 3D terrain: 1. Coulomb mixture theory. Journal of Geophysical Research 106(B1): 537–552.

Jiang L, LeBlond PH 1993. Numerical modeling of an underwater Bingham plastic mudslide and the waves which it generates. Journal of Geophysical Research 98(C6): 10303–10317.

Jiang L, LeBlond PH 1994. Three-dimensional modeling of tsunami generation due to a submarine mudslide. Journal of Physical Oceanography 24(3): 559–572.

Keller GH, Bennett RH 1970. Variations in the mass physical properties of selected submarine sediments. Marine Geology 9: 215–223.

Lee HJ, Edwards BD 1986. Regional method to assess offshore slope stability. Journal of Geotechnical Engineering 112: 489–510.

Lewis K 1994. The 1,500 km long Hikurangi Channel: an axial channel that escapes its trench, crosses a plateau and feeds and fan-drift. Geo-Marine Letters 14: 19–28.

Lewis K 1998. Kaikoura Canyon: sediment conduit to the deep. Water & Atmosphere 6(2): 24–25.

Lewis K, Barnes PM 1999. Kaikoura Canyon, New Zealand: active sediment conduit from near-shore sediment zones to trench-axis channel. Marine Geology 162: 39–69.

Lewis K, Collot J-Y 2001. Giant submarine avalanche: was this "Deep Impact" New Zealand style? Water & Atmosphere 9: 26–27.

Lewis K, Pantin HM 2002. Channel-axis, overbank and drift sediment waves in the southern Hikurangi Trough, New Zealand. Marine Geology 192: 123–151.

Lewis K, Pettinga JR 1993. The emerging, imbricated frontal wedge of the Hikurangi margin. In: Balance PF ed. South Pacific Sedimentary Basins: sedimentary basins of the world, 2. New York, Elsevier Science. Pp. 225–250.

Lewis K, Collot J-Y, Lallemand SE 1998. The dammed Hikurangi Trough: a channel-fed trench blocked by subducting seamounts and their wake avalanches (New Zealand–France GeodyNZ). Basin Research 10: 441–468.

Liu PL-F, Wu T-S, Raichlen F, Synolakis CE, Borrero JC 2005. Runup and rundown generated by three-dimensional sliding masses. Journal of Fluid Mechanics 536: 107–144.

Nichol S, Goff J, Regnauld H 2003. Cobbles to diatoms: facies variability in a paleo-tsunami deposit. Proceedings of the Coastal Sediments 2003 "Crossing Disciplinary Boundaries". The Fifth International Symposium on Coastal Engineering and Science of Coastal Sediment Processes. Florida, United States. Pp. 1–11.

Nicol A 1991. Structural styles and kinematics of deformation on the edge of the New Zealand plate boundary zone, mid Waipara region, North Canterbury. Unpublished PhD thesis, University of Canterbury, Christchurch, New Zealand.

Norris RJ, Koons PO, Cooper AF 1990. The obliquely-convergent plate boundary in the South Island of New Zealand: implications for ancient collision zones. Journal of Structural Geology 12: 715–725.

Pettinga JR, Yetton MD, Van Dissen RJ, Downes G 2001. Earthquake source identification and characterisation for the Canterbury region, South Island, New Zealand. Bulletin of the New Zealand Society for Earthquake Engineering 34: 282–317.

Reyners M, Cowan HA 1993. The transition from subduction to continental collision: Crustal structure in the north Canterbury region, New Zealand. Geophysical Journal International 125: 1224–1236.

Reyners M, Robinson R, McGinty P 1997. Plate coupling in the northern South Island and southernmost North Island, New Zealand, as illuminated by earthquake focal mechanisms. Journal of Geophysical Research 102: 15197–15210.

Rzadkiewicz SA, Mariotti C, Heinrich P 1997. Numerical simulation of submarine landslides and their hydraulic effects. Journal of Waterway, Port, Coastal, and Ocean Engineering 123: 149–157.

Savage SB, Hutter K 1989. The motion of a finite mass of granular material down a rough incline. Journal of Fluid Mechanics 199: 177–215.

Shepard FP 1981. Submarine canyons: multiple causes and long- time persistence. American Association of Petroleum Geologists Bulletin 65: 1062–1077.

Stirling M, Pettinga JR, Berryman K, Yetton MD 2001. Probabilistic seismic hazard assessment of the Canterbury region, New Zealand. Bulletin of the New Zealand Society for Earthquake Engineering 34: 318–334.

US Army Corps of Engineers 1998. Coastal Engineering Manual, Part III, Chapter 5. Erosion, transport, and deposition of cohesive sediments. Department of the Army, Washington DC, United States. 64 p.

Van Dissen R 1991. An evaluation of seismic hazard in the Kaikoura region, southeastern Marlborough: New Zealand. Geological Survey Record 43: 93–99.

Van Dissen RJ, Berryman KR 1996. Surface rupture earthquakes over the last ~1000 years in the Wellington region, New Zealand, and implications for ground shaking hazard. Journal of Geophysical Research 101: 5999–6019.

Van Dissen R, Yeats RS 1991. Hope fault, Jordan thrust, and uplift of the seaward Kaikoura Range, New Zealand. Geology 19: 393–396.

Walcott RI 1978. Present tectonics and late Cenozoic evolution of New Zealand. Geophysical Journal of the Royal Astronomical Society 52: 137–164.

Walters RA 2004. Tsunami generation, propagation, and runup. In: Spaulding ML ed. Estuarine and Coastal Modeling. Proceedings of the 8th International Conference, American Society of Civil Engineers. Pp. 423–438.

Walters RA 2005a. Coastal Ocean models: two useful finite element methods. Continental Shelf Research 25(7–8): 775–793.

Walters RA 2005b. A semi-implicit finite element model for non-hydrostatic (dispersive) surface waves. International Journal of Numerical Methods in Fluids 49: 721–737.

Walters RA, Casulli, V 1998. A robust, finite element model for hydrostatic surface water flows. Communications in Numerical Methods in Engineering 14: 931–940.

Walters RA, Barnes P, Goff J 2006. Locally generated tsunami along the Kaikoura coastal margin: Part 1. Fault ruptures. New Zealand Journal of Marine and Freshwater Research 40: 1–16.

Walters R, Wild M, Fleming J, Hurren H, Duncan M, Willsman A 2004. Kaikoura District engineering lifelines project: tsunami hazard assessment (Part 1b). National Institute of Water and Atmospheric Research Ltd. 82 p.

Watts P 1998. Wavemaker curves for tsunamis generated by underwater landslides. Journal of Waterway, Port, Coastal, and Ocean Engineering 124: 127–137.

Watts P, Imamura F, Grilli ST 2000. Comparing model simulations of three benchmark tsunami generation cases. Journal of Scientific Tsunami Hazards 18(2): 107–123.